

THE FORMATION OF SWIRL DEFECTS IN SILICON BY AGGLOMERATION OF SELF-INTERSTITIALS

H. FÖLL * and U. GÖSELE **

Max-Planck-Institut für Metallforschung, Institut für Physik, Büsnauer Strasse 171, D-7000 Stuttgart 80, Germany

and

B.O. KOLBESEN

Siemens AG, Grundlagenentwicklung Halbleiter, P.O. Box 460705, D-8000 München 46, Germany

Received 19 January 1977

Through recent electron microscope investigations it is now well established that A-swirl defects in float-zone grown silicon crystals are dislocation loops of interstitial type which are formed by the agglomeration of silicon self-interstitials. In the first part the origin of the silicon self-interstitials is discussed: the “non-equilibrium interstitial model” invoked by Petroff and De Kock and the “equilibrium interstitial model” proposed by Föll et al. are contrasted. It is shown that only the “equilibrium interstitial model” is compatible to all the experimental facts of swirl defects known up to now. In the second part a general model for the formation of swirl defects is presented. The basic idea of this model is the assumption that A-swirl defects are generated by the collapse of B-swirl defects. B-swirl defects are assumed to be droplet-like agglomerates of silicon self-interstitials and some impurity atoms, particularly carbon, which govern the growth kinetics and stability of B-swirl defects. Thermodynamic considerations are presented, which in the case of A-swirl defects are relatively simple and straightforward, whereas those for the B-swirl defects are more sophisticated and include several speculative assumptions. This model is able to interpret all swirl data known so far, especially the dependence of the occurrence of swirl defects on the growth rate and the dependence of the swirl properties on the carbon concentration.

Introduction

During the cooling of as-grown, dislocation-free, high-purity silicon crystals, point defect agglomerates are often formed. Two types of these agglomerates (usually named “swirl defects”) differing in size, density and spatial distribution may occur simultaneously [1]. Following De Kock [1] the larger ones are termed “A-swirl defects” (briefly “A-defects”), the smaller ones “B-swirl defects” (briefly “B-defects”). In this paper the name “swirl defect” will be used exclusively for the defects in float-zoned material

with small impurity contents ($O \lesssim 10^{16} \text{ cm}^{-3}$, $C \lesssim 10^{17} \text{ cm}^{-3}$, $Cu \lesssim 10^{12} \text{ cm}^{-3}$, $Au \lesssim 10^9 \text{ cm}^{-3}$), because in other material “swirls” are expected to be rather precipitates of impurities than point defect agglomerates. In analogy to metals, in which vacancies are the dominant point defects in thermal equilibrium (see e.g. ref. [2], in the past it was generally assumed that swirl defects are formed by agglomeration of the vacancies [1,3–8] which are present in thermal equilibrium near the melting point, since these are unable to find sinks for annealing during cooling. This is so because the crystals neither contain dislocations nor are they thin enough for the surface to act as an efficient sink for point defects. However, in 1975 two research groups independently and almost simultaneously demonstrated by means of transmission electron microscopy combined with a special specimen preparation technique [9]) that at least the A-defects are dislocation loops or clusters of

* Present address: Department of Materials Science and Engineering, College of Engineering, Bard Hall, Cornell University, Ithaca, New York 14853, USA.

** Present address: Atomic Energy Board, Physical Metallurgy Division, Private Bag X256, Pretoria 0001, South Africa.

dislocation loops [8,10] (so-called “swirl loops”), which are formed by the agglomeration of silicon *self-interstitials* [11–17]. A corresponding experimental proof of the nature and the type of the B-defects has not yet been possible [14,15]. Indirect arguments led to the conclusion that B-defects are *not* (small) dislocation loops but loosely packed, three-dimensional agglomerates of silicon self-interstitials and some impurity atoms [14].

In order to understand the nature and the formation of swirl defects in silicon, it is helpful to consider two aspects of the subject matter separately:

(i) The relationship between swirls and silicon self-interstitials, i.e. the *origin* of *interstitial-type* dislocation loops.

(ii) The *nucleation* and *formation* of the swirls, i.e., how the sensitive dependence of swirl properties (e.g., occurrence, density and size) on growth conditions and impurity content can be understood.

These items are linked by the question of the origin of the self-interstitials, since any model dealing with item (ii) has to start at this point. Two models concerning this question are under discussion, the “non-equilibrium interstitial model” invoked by Petroff and De Kock [15] (formerly used by De Kock et al. for vacancies [4,6]) and the “equilibrium interstitial model” proposed by Föll et al. [13, 14] and Seeger et al. [17]. The first model, which follows the theories of Fletcher [18,19] and Webb [20], suggests that silicon self-interstitials may be trapped during crystal growth at the solid–liquid interface and finally be incorporated into the crystal in non-equilibrium concentrations. Nevertheless in this model the equilibrium point defect is assumed to be the vacancy.

By contrast, the alternative model proposes that in silicon *not* the vacancies but the self-interstitials are the dominating equilibrium point defects at high temperatures. This assumption is based on the evaluation of self-diffusion, quenching and radiation damage experiments on silicon [21–25].

With respect to the *formation* of swirl defects, the first general model that included all observations on swirl defects known at that time was given in De Kock’s fundamental work [1]. In the meantime this model (which was based on the assumption of an independent formation of both A- and B-defects by vacancy–oxygen agglomeration) has been demon-

strated to be untenable as to all its essential points [4,6,11–17]. In recent papers [6,14–17] it has been assumed that A-defects (i.e. interstitial-type dislocation loops) result from a collapse of B-defects (i.e. loose, three-dimensional agglomerates of interstitials). We shall briefly call this hypothesis the “B-collapse model”. However, so far this model is merely a basic idea and too general to account for all experimental observations.

The aim of the present paper is two-fold: Firstly, we shall contrast the equilibrium interstitial model and the non-equilibrium interstitial model and, because of their importance, discuss this issue in some detail. In the second and main part of the paper we shall discuss the general conditions which must be fulfilled in order to make the B-collapse model work at all. By considering a large body of experiments including new ones presented in this paper – we finally arrive at a detailed picture of swirl formation on the basis of the B-collapse model. It should be emphasized, however, that this model has to be regarded as a first step in the understanding of the formation of swirl defects in silicon. Though it is sophisticated enough, nature appears to be even more complicated.

2. Brief summary of the experimental results on the formation of swirl defects

The following items are extracted from numerous papers [1,4–7,12–17,26] and, in the opinion of the present authors, may be regarded as reliable experimental findings. Together with the observations concerning the rôle of impurities (see section 4) they give the framework of facts which a swirl formation model has to account for and supply the possibility to exclude one of the competitive models for the origin of the silicon self-interstitials.

(i) Observations at “high” growth rates v_0 (i.e. $v_0 \lesssim 2$ mm/min): A-defects disappear suddenly at $v_0 \approx 4$ mm/min, B-defects disappear at $v_0 \approx 5$ mm/min [4,6,14], the actual limit of v_0 slightly depending on the crystal diameter [4,6,14] and the carbon content (see section 4).

(ii) Observations at “low” growth rates ($v_0 \lesssim 2$ mm/min: in crystals with 23 mm diameter both A-defects and B-defects disappear at growth rates below $v_0 \approx 0.2$ mm/min [26].

(iii) If a crystal is pulled at a growth rate at which swirls are normally not present (present) and cooled down at a cooling rate corresponding to a growth rate at which swirls normally are present (not present), swirls are always found to be present (not present) [6,26].

(iv) B-defects are not observed in vacuum-grown crystals [1] or in argon-grown crystals with a low impurity content (see section 4).

(v) With increasing v_0 the distance d_B between B-defects and the rim of the crystal firstly decreases (for $v_0 \leq 1$ mm/min) and increases again with further increasing v_0 . The distance d_A between A-defects and the rim shows a similar behaviour as d_B , however, $d_A > d_B$ always holds [6,14,26].

(vi) The central region of a crystal often shows a strongly reduced density of B-defects and is often completely B-defect free, the diameter of this region decreases with increasing growth rate [27].

3. Swirl defects and silicon self-interstitials

Nowadays it is well established that swirl defects arise from the *condensation* of silicon *self-interstitials*. Recent counterstatements which considered swirls to originate either from different mechanisms (e.g., prismatic loop punching) or to be associated with impurities [12,28,29], in the opinion of the present writers have been disproved convincingly [14–17,30]. The origin of the interstitials has so far been the only open question. Before discussing the implications of the two models mentioned in section 1, we shall present them in more detail.

(i) The equilibrium interstitial model. This model is based on a good deal of different experiments (see, e.g., refs. [17,25]) that lead to the conclusion that at high temperatures self-diffusion is governed by self-interstitials and that self-interstitials are the dominating point defects in thermal equilibrium near the melting point. An evaluation of a number of experiments, including swirl investigations, lead to the following properties of the high-temperature configuration of the silicon self-interstitial at the melting temperature T_m [17]: formation enthalpy $H_1^F = 3.04$ eV, formation entropy $S_1^F = 6.11 k$ ($k =$ Boltzmann's constant), migration enthalpy $H_1^M = 2.0$ eV, migration entropy $S_1^M = 6.96 k$. Thus at $T = T_m$ the concentra-

tion of interstitials is $2 \times 10^{16} \text{ cm}^{-3}$ and the diffusion coefficient $D_1(T_m) = 4.29 \times 10^{-6} \text{ cm}^2/\text{s}$ [17]. The high formation and migration entropy indicates that the interstitial is "extended", i.e., a crystal region which in the perfect crystal contains about 10 atoms comprises 11 atoms if it hosts an interstitial [21–23] (see also section 6).

(ii) The non-equilibrium interstitial model. In this model it is assumed that during the growth of a crystal a certain number, n_S , of silicon self-interstitials are trapped at the solid–liquid interface. The theory of this process [20] gives the number Δn of the excess interstitials (with respect to the equilibrium concentration) finally incorporated in the bulk to be

$$\Delta n = \frac{n_S - n(T_m)}{1 + [D_1(T_m)/v_{\text{mic}}]\delta}, \quad (1)$$

with v_{mic} = microscopic growth rate in growth direction (i.e. $v_{\text{mic}} > 0$), δ = thickness of the diffuse interface [20], see also ref. [6], $n(T_m)$ = equilibrium number of interstitials at T_m . Because δ and especially n_S are unknown, a quantitative evaluation of eq. (1) is useless and furthermore aggravated by the unknown number of excess interstitials recombining with vacancies, which in this model are assumed to be the equilibrium defects.

We now discuss the consequences of the two models on swirl formation. In the equilibrium interstitial model the number of interstitials present near the melting point is independent of the growth conditions. All that need be done was to prove whether the equilibrium concentration and the diffusion coefficient of the interstitials estimated from swirl experiments are in accord with the theoretical predictions. This is indeed the case, as has been shown in [13,17].

The situation is completely different regarding the non-equilibrium interstitial model. The number of interstitials present near the melting point, Δn , depends on v_{mic} ; v_{mic} in turn is a function of growth parameters and approximately given by

$$v_{\text{mic}} = v_0(1 - \alpha \cos 2\pi R t), \quad (2)$$

with

$$\alpha = 2\pi R \Delta T / M v_0 \quad (3)$$

($R =$ crystal rotation rate, $t =$ time, $\Delta T =$ temperature variation of a given point of the interface during one seed revolution, $M =$ temperature gradient in the melt

adjacent to the interface [31]. For the *mean* microscopic growth rate *in growth direction*, \bar{v}_{mic} , which determines the *mean* excess number of silicon interstitials, follows from eq. (2)

$$\bar{v}_{\text{mic}} = \begin{cases} \frac{v_0}{1 - 1/\pi \arccos(1/\alpha)} \\ \text{for } \alpha > 1, \text{ i.e. remelt conditions,} \\ v_0 \\ \text{for } \alpha < 1, \text{ i.e. no-remelt conditions.} \end{cases} \quad (4)$$

For the temporary maximum \hat{v}_{mic} of v_{mic} , which determines the local maximum of Δn , one obtains,

$$\hat{v}_{\text{mic}} = v_0 + 2\pi R \Delta T / M. \quad (5)$$

According to eq. (1), Δn increases with increasing v_{mic} . Swirl defects, however, vanish with increasing v_0 . This was attributed by De Kock et al. [4,6] and Petroff and De Kock [15] to a decrease of \bar{v}_{mic} with increasing v_0 in the v_0 region where remelt processes (i.e. $\alpha > 1$) are suppressed (i.e. $\alpha < 1$). The dependence of \bar{v}_{mic} and \hat{v}_{mic} on v_0 is shown in fig. 1. It can be seen that there is only a very small decrease of

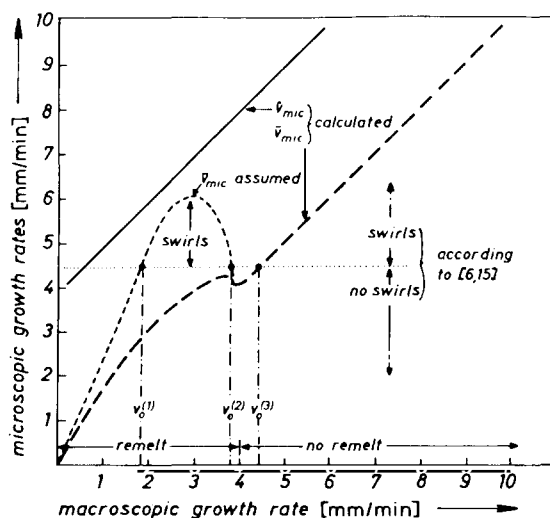


Fig. 1. Dependence of \bar{v}_{mic} and \hat{v}_{mic} on v_0 . The calculated curves and one assumed curve for \bar{v}_{mic} are given. No remelt conditions were assumed to be present at $v_0 \geq 4$ mm/min. The growth rate regions where swirls should not occur according to refs. [6,15] are shown.

\bar{v}_{mic} at $v_0 \approx 4$ mm/min (no-remelt conditions were assumed at $v_0 = 4$ mm/min), whereas \hat{v}_{mic} increases monotonically. It is true that \bar{v}_{mic} is larger than v_0 in the remelt region (with a maximum value of $\bar{v}_{\text{mic}}/v_0 = 2.0$ for $v_0 \rightarrow 0$, but theory gives no convincing reason why swirls should disappear at $v_0 \approx 4$ mm/min and at higher growth rates because of a lack of excess interstitials. Nevertheless, let us assume that \bar{v}_{mic} in fact would decrease remarkably if remelt is suppressed, e.g. by a suitable dependence of M , ΔT or δ on v_0 , resulting in the dashed \bar{v}_{mic} curve in fig. 1. Thus, according to refs. [4,6,15], a minimum value of Δn , and consequently of \bar{v}_{mic} , must exist below which no swirl defects should be observed. From fig. 1 it can be seen that consequently swirl defects should be absent for $0 \leq v_0 \leq v_0^{(1)}$, $v_0^{(2)} \leq v_0 \leq v_0^{(3)}$ and that swirl defects should be present at $v_0 \geq v_0^{(3)}$. Neither is this observed nor do swirls re-occur at high growth rates [4] nor do they vanish at moderate v_0 .

If remelt suppression would influence Δn and hence the swirl density via a change in \bar{v}_{mic} , a reduction of the crystal rotation rate R should give the same effect as an increase of v_0 (cf. eq. (3)). This is not observed, the swirl density remains constant in a large R interval ($3 \leq R \leq 60 \text{ min}^{-1}$) for $v_0 = 3$ mm/min, only at $v_0 = 4$ mm/min (where A-defects just are disappearing) the A-defect density is somewhat influenced by R , whereas the B-defect density remains constant [4].

Altogether the sudden disappearance of A- and B-defects at high growth rates, which was regarded as strong evidence for the validity of the non-equilibrium interstitial model [4,6,15], is by no means a consequence of this model.

According to the non-equilibrium interstitial model, very little excess interstitials are incorporated for very low growth rates, (at low but finite growth rates even $\Delta n = 0$ should hold because of the recombination of excess interstitials with vacancies) swirl defects consequently should not be observed at all. This indeed was found by Roksnøer et al. [26]; swirl defects disappear at $v_0 \leq 0.2$ mm/min (for crystals with a diameter of 23 mm). However, this is not due to a lack of interstitials but due to the outdiffusion of interstitials to the surface, as unambiguously shown in ref. [26]. The observation that a crystal grown at $v_0 = 0.2$ mm/min (hence swirl-free) again contains swirls in parts which are cooled down rapidly enough

[26], is an unambiguous demonstration that in principle sufficient interstitials are present to form swirls.

Further arguments against the non-equilibrium interstitial model are given by de Kock in his earlier work [1] and hold, although put forward for vacancies, in the case of interstitials, too.

In summary, we state that neither theory nor experiments support the non-equilibrium model. Although being a possibility, an excess trapping of interstitials appears to play no essential rôle in conventionally grown silicon crystals. We arrive thus at the conclusion that the equilibrium interstitial model is valid and adopt in the following the data given at the beginning of this section.

4. The rôle of impurities in the formation of swirl defects; experimental observations and discussion

We restrict ourselves to the rôle of oxygen and carbon, which usually are the dominating impurities in float-zoned silicon. Fast diffusing metals, e.g., Cu or Au, may result in a decoration of A- and B-defects as well [12], but apparently do not influence the formation of swirl defects. Hydrogen, which has found some interest because it can prevent swirl formation at lower growth rates as normally necessary for this purpose [1], introduces a number of other phenomena, quite unclear up to now [1,32], and will not be considered in this paper.

The experimental findings which suggest an influence of oxygen and especially of carbon on swirl formation are:

- (i) The inhomogeneous distribution of the swirl defects (in the "swirl" pattern), which, as shown in section 3, cannot be accounted for by an inhomogeneous incorporation of the silicon self-interstitials, suggests a heterogeneous nucleation of swirls at inhomogeneously incorporated impurities.
- (ii) The decrease in the density of B-defects and their final disappearance with decreasing carbon content [27].
- (iii) The increase of size and complexity of the swirl loops with decreasing impurity content (see below).

We will consider these items in more detail. Ad (i). Recent experiments by Kamm and Müller [33] show that swirls are always formed at those

crystal sites at which the local maxima of the phosphorus concentration occur. Because phosphorus cannot act as nucleus in the swirl formation (swirls are observed in undoped as well as in p-type material), the impurity responsible for the nucleation of the swirls like phosphorus must have a distribution coefficient $k < 1$ (for the definition of k see ref. [34]) and must be present in all crystals in noticeable quantities. Carbon meets both conditions ($k_C = 0.05$ [35]), whereas oxygen has a distribution coefficient close to unity [7,36]. Hence, carbon is most likely the impurity which governs the nucleation of swirl defects.

Ad (ii). It is known that in vacuum-grown crystals, which thus contain very little amounts of impurities, no B-defects are found [1]. This could be also confirmed for two vacuum-grown crystals by the present authors. A new observation is the absence of B-defects in argon-grown crystals with very low impurity content (crystals AZ 6 and AZ 7, see table 1). Observations of occurrence, density, size and complexity of A- and B-defects in a number of different crystals are summarized in table 1. Again, carbon appears to influence the swirl parameters more than oxygen. Ad (iii). Fig. 2. shows some swirl loops which may be considered typical for the different classes listed in table 1. It is of particular interest that the swirl loops in AZ 7 are practically identical with those observed in vacuum-grown material (see ref. [14]), especially the "small loops" [14] decorating the large dislocations are found in this crystal, too. It should be emphasized, however, that even in specimens prepared from the same crystal, size and complexity of the swirl loops differ considerably. This holds even for a single sample. The typical sizes and the degree of complexity given in table 1 must therefore be regarded as approximate values obtained by evaluating some hundred swirl loops and should only give an impression of what is found.

In ref. [14] a model was presented which explains the increase in complexity of the swirl loops with decreasing impurity content by a loop multiplication process driven by impurities such as carbon or oxygen. Our new results, especially the difference in complexity of the swirl loops in crystals AZ 7, AZ 5 and AZ 3 (with about the same oxygen content), suggest an increase of the temperature below which A-defects are formed with decreasing carbon content. Thus in very pure crystals the multiplication process may

Table 1
Properties of the crystals investigated

Crystal ^a	Diam.	Conductivity Resistivity		Growth direction	Growth rate (mm/min)	Content of		Swirl density ^b		TEM results	
		Type	(Ω cm)			Oxygen (cm^{-3})	Carbon (cm^{-3})	A-defects (cm^{-3})	B-defects (cm^{-3})	Size (μm)	Classification ^c
AZ 1 ^d	34	n	60	111	3.0	10^{15}	10^{16}	10^9	$2-5 \times 10^{10}$	2-5	2, 3
AZ 2 ^d	34	n	70	111	3.0	5×10^{15}	5×10^{16}	10^9	$2-3 \times 10^{11}$	0.5-2	1, 2, (5)
AZ 3 ^d	34	p	7000	111	2.0	6×10^{15}	1.2×10^{17}	5×10^8	5×10^{10}	1-2.5	1, 2, 5
					2.5			10^{11}		0.5-2.5	1, 2, 5
					3.0			10^9	$2-3 \times 10^{11}$	0.5-2	1, 2, 5
					3.5			10^8	$2-3 \times 10^{11}$	0.5-2	1, 2, 5
					4.0			None	5×10^{10}	0.5-1	1, 2, 5
					4.5			None	None	-	-
					5.0			None	None	-	-
AZ 4	33	n	1	111	3.0	1.5×10^{16}	10^{16}	$0.5-1 \times 10^9$	$1-3 \times 10^{10}$	-	Only few micrographs
AZ 5	33	n	1	111	1.5 ^e	10^{16}	2×10^{16}	Dislocations	-	-	-
					2.0			10^8	$0.2-1 \times 10^{10}$	2-4	(1), 2, 3
					3.0			10^8	1.5×10^{10}	1-2	2, 3
					4.0			None	None	-	-
AZ 6	33	n	9	100	2.0 ^e	1.4×10^{16}	5×10^{15}	$0.5-1 \times 10^8$	None	No TEM	-
					3.0			$0.5-1 \times 10^8$	None	1-3	2, 3
					4.0			None	None	-	-
AZ 7	33	n	46	100	2.0 ^e	8×10^{15}	6×10^{15}	$1-3 \times 10^8$	None	2-30	3, 4
					3.0			$1-3 \times 10^8$	None	2-6	2, 3, 4
					4.0			None	None	-	-
VZ 1 ^d	34	n	60	111	1.8	$<5 \times 10^{13}$	$<2 \times 10^{15}$	10^7-10^8	None	3-40	4
VZ 2	40	n	5000	111	2.5	$<5 \times 10^{14}$	$<2 \times 10^{15}$	10^7-10^8	None	2-5	2, 3, (4)

^a AZ and VZ refer to crystals float-zoned in argon or vacuum, respectively.

^b The density values were determined after etching (cf. ref. [38]) in well-developed swirl-bands.

^c The following classification scheme is used: (1) single loops, (2) simple loop arrangements, (3) complicated loop arrangements, (4) large and highly complicated loop arrangements, (5) loops or loop arrangements including stacking faults. Italics refer to the most typical defects, parentheses to seldom observed defects.

^d These crystals have already been discussed in ref. [14].

^e At these growth rates, dislocations were introduced.

^f In this crystal, B defects were only found in one swirl band near the rim of the crystal.

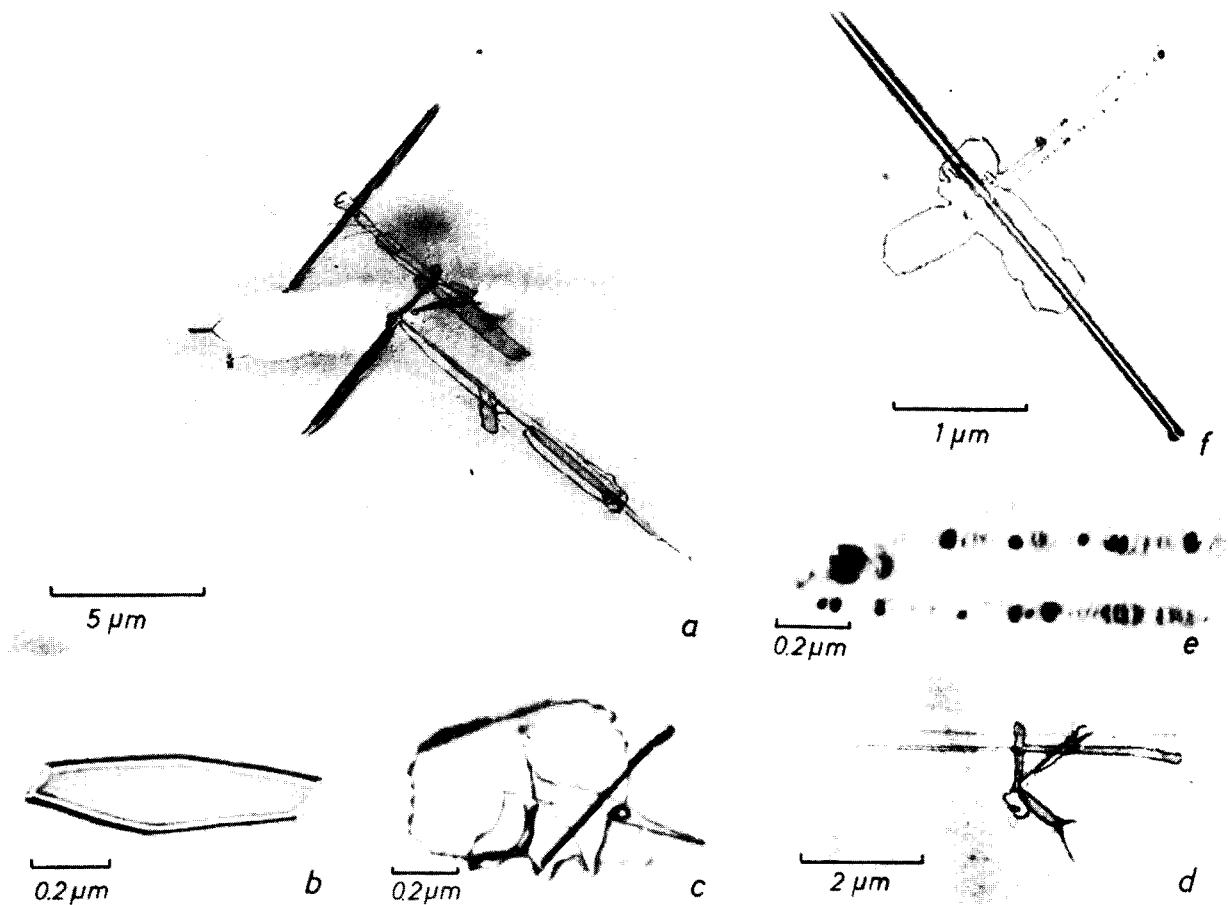


Fig. 2. Selected examples of swirl loops. These micrographs, together with the micrographs shown in refs. [14,17] may give an impression of the variety of swirl loops observed: (a) is an example for a large and highly complicated swirl loop (classification 4), (b) and (c) show a faulted loop (classification 5) and a simple loop arrangement (classification 2); (d) and (f) may give an impression of complicated loop arrangements (classification 3); (e) finally is an enlarged part of (f) showing the small loops of the decoration.

occur more frequently, making the swirl loops more complex.

5. Thermodynamic consideration of A-swirl defects

All A-defects examined in the electron microscope have been found to be dislocation loops or clusters of dislocation loops with diameters $>0.3 \mu\text{m}$. Defects of this size are safely detected by etching or by X-ray topography after decoration. The absence of, e.g., the typical A-defect etch pits after a Sirtl-etch [37,38]

hence must not be explained by the presence of A-defects which are too small to be detected (as it may be the case with B-defects), but reflects in fact the absence of A-defects.

A model of the growth of A-defects after small faulted dislocation loops have been formed is given in ref. [14]. Here we are interested in the formation of the embryonic loop. In the following we consider A-defects therefore as small faulted single dislocation loops.

The thermodynamic situation of a crystal without sinks for point defect annealing is as follows: At $T =$

T_m an equilibrium concentration of interstitials is present which gives (by definition) the lowest free enthalpy $G_r(T_m)$ * possible. In the absence of dislocations which can act as sinks and neglecting annealing at the surface for the time being, the total number of interstitials (including those in agglomerates) remains constant during the cooling of the crystal. Thus at $T < T_m$ a supersaturation of interstitials is present, leading to a free enthalpy $G_r(T)$ that is larger than $G_r(T)$ at equilibrium conditions. The formation of an interstitial agglomerate which contains n_a interstitials at a certain temperature may result in a lowering of the free enthalpy $G_a(n_a, T)$ of the crystal and may therefore be thermodynamically favoured. The quantity of interest is the difference $\Delta G_a(n_a, T) = G_r(T) - G_a(n_a, T)$ of the free enthalpies of the crystal if either all interstitials are distributed randomly (free enthalpy = $G_r(T)$) or n_a interstitials are incorporated in an agglomerate (free enthalpy = $G_a(n_a, T)$), the remaining interstitials being furtheron distributed at random. If the agglomerate formed is an A-defect, i.e. a small faulted dislocation loop including a stacking fault, we approximately arrive at

$$\Delta G_1 \approx -H_1^F(1 - T/T_m)n_1 + \mu[b^2r_1/2(1 - \nu)] [\ln(r_1/b) + 5/3] + \pi r_1^2 \gamma. \quad (6)$$

For the derivation of this equation and the meaning of the symbols see the appendix. This function is plotted in fig. 3 for various temperatures T . The essential point derivable from fig. 3 is that a loop formed by less than n_1^{\min} atoms (see fig. 3) would increase ΔG_1 while growing and would thus be not stable but shrink. Growth of a loop is only possible if $n_1 \geq n_1^{\min}$ or generally, if $\partial \Delta G_1 / \partial n_1 \leq 0$. Fig. 4 shows n_1^{\min} versus T according to eq. (6). It is worthwhile to note that for smaller supersaturations (e.g., because a fraction of the interstitials present at T_m anneals by outdiffusion to the surface) at a given temperature larger n_1^{\min} values result. More detailed calculations and discussions may be found in refs. [39–41]; see also ref. [1]. Here we want to demon-

* The indices “r” and “a” in this and the following sections refer to interstitials which are randomly distributed or incorporated into an agglomerate; “l” and “d” refer to special forms of agglomerates, namely dislocation loops and droplets (see below).

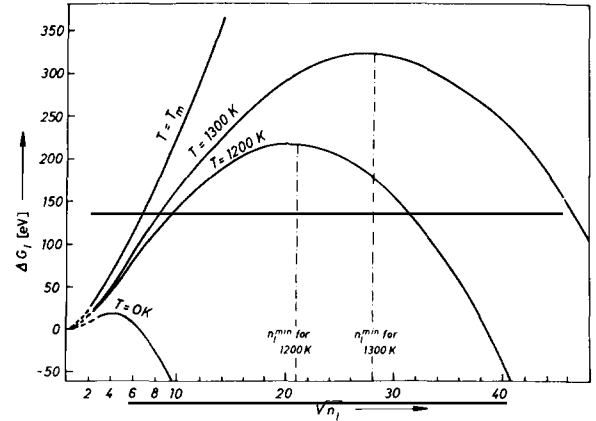


Fig. 3. The change in the free enthalpy of a crystal containing $n(T_m)$ interstitials if a (faulted) dislocation loop containing n_1 interstitials is formed.

strate by simple calculations the general line of reasoning. The important conclusion which can be drawn from fig. 4 is that even at relatively low temperatures the formation of dislocation loops requires very large nuclei. Thus the “direct” formation of interstitial-type dislocation loops in silicon is unlikely, a certain kind of “forerunners” of considerable size are required for their formation.

The situation is completely different from what is known from metals. Generally n_1^{\min} is much smaller. Furtheron, vacancies are the equilibrium defects, quenching experiments therefore result in the formation of vacancy-type dislocation loops or voids. The nuclei for these dislocation loops are thought to be

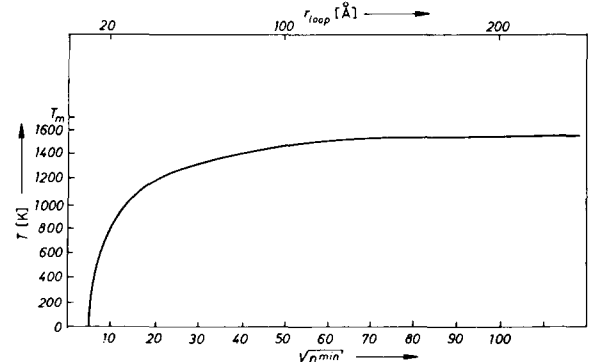


Fig. 4. Critical number n_1^{\min} of interstitial atoms necessary for the origination of a dislocation loop able to grow.

almost stress free vacancy platelets cf. refs. [39–41] – a corresponding nucleus for interstitial-type loops cannot exist.

6. Properties of B-swirl defects

The nature of B-defects has not yet been established experimentally. Electron microscope investigations led to the alternatives that B-defects are either very small dislocation loops or a kind of agglomerates without a strong strain field [14,15]. Experimental and theoretical findings strongly support the second possibility [14,15]. We adopt the concept that B-defects are almost stress free three-dimensional agglomerates of silicon self-interstitials, but we must give a more definite idea of the B-defects in order to be able to consider the thermodynamics and growth kinetics of these defects.

Contrary to A-defects, in this model B-defects may have any small size. One hence must expect that B-defects below a certain size are *not* detected by etching or by X-ray topography after decoration. Our feeling is that the detection limit for etching lies around 1000 interstitial atoms per B-defect. The non-occurrence of B-defects thus does not necessarily imply that no B-defects are present, but reflects rather that they are too small to be detected. In particular, the disappearance of B-defects with increasing growth rate may consequently be interpreted by a continuous decrease of their sizes.

The formation of a stress-free agglomerate of silicon self-interstitials could be conceived according to the following recipe: Take out of the crystal $10n_a$ atoms and fill the hole produced with *liquid* silicon. Because of the 10% higher density of liquid silicon compared to crystalline silicon, such a “droplet” inside the crystal lattice would have an interstitial-agglomerate nature and contains just n_a (henceforth n_d) interstitial atoms. The “extended interstitial” proposed by Seeger and coworkers [21–25] (see also section 3) may be regarded as a droplet of one interstitial. It is hence suggestive that larger droplets can be formed by the agglomeration of extended interstitials. Such droplets would be relatively stress-free and indeed hard to detect in the electron microscope.

The “interstitial atoms” in a droplet must not be identified with distinct atoms, they are rather

“smeared out”, leading to the high formation entropy of extended interstitials as well as of droplets.

For a thermodynamic description in the way outlined in section 5 we firstly need the free enthalpy $G_d = H_d - TS_d$ of the droplet as a function of the number of interstitials in the droplet and the temperature T . We consider two extreme cases:

(i) The single extended interstitial which may be considered as a droplet with $n_d = 1$. Thus $H_d = H_1^F$ and $S_d = S_1^F$ holds, leading to $G_d(n_d = 1, T) = H_1^F - TS_1^F$.
(ii) Large agglomerates. They may be regarded as real droplets. Neglecting the surface (or better interface) energy we have $G_d = n_d(H_{HF} - TS_{HF})$, with H_{HF} = heat of fusion per interstitial atom and $S_{HF} = H_{HF}/T_m$ = entropy of fusion per interstitial atom.

Inserting numbers ($H_1^F = 3$ eV, $S_1^F = 6$ k, see section 3; $H_{HF} \approx 4.1$ eV, $S_{HF} \approx 28.1$ k [42]) we recognize that $\partial G_d/\partial n_d$ must depend on n_d in order to account for the two extreme cases. As in section 5 we are interested in $\Delta G(n_d, T)$ or in $\partial \Delta G_d/\partial n_d$; considerations similar to those in section 5 (see the appendix) lead to

$$\begin{aligned} \partial \Delta G_d/\partial n_d \approx \partial H_d/\partial n_d - H_1^F(1 - T/T_m) \\ - T\partial S_d/\partial n_d. \end{aligned} \quad (7)$$

The quantities $\partial H_d/\partial n_d$ and $\partial S_d/\partial n_d$ are the binding enthalpy and the binding entropy, respectively, of an (extended) interstitial to a droplet speaking in terms of agglomeration of single point defects. At present their theoretical calculation is hardly possible and would be furthermore aggravated by a (unknown) temperature dependence of H_d and especially of S_d which should be taken into consideration. In order to obtain a stable droplet at all, the growth condition $T\partial S_d/\partial n_d \geq \partial H_d/\partial n_d$ (corresponding to $\partial \Delta G_d/\partial n_d \leq 0$) must hold at least for $n_d^{\min} \leq n_d \leq n_d^{\max}$. Here, n_d^{\min} gives the critical size of the nucleus required for a droplet, n_d^{\max} the equilibrium size.

Fig. 5 may serve to illustrate eq. (7). Firstly, let us discuss the curves corresponding to the enthalpy and entropy term of eq. (7) for $T = T_m$ (briefly called enthalpy and entropy curves). Between the extreme cases for very small and very large droplets these curves are given tentatively. n_d^{\min} is given by the cross-point of the two curves; n_d^{\max} is not defined in the approximation used at $T = T_m$. This is due to the neglecting of an additional entropy term in eq. (7).

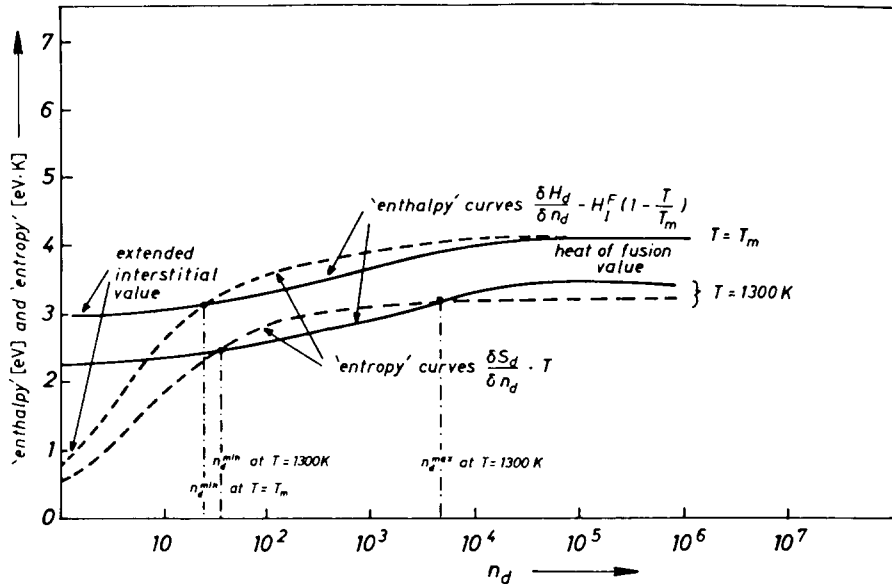


Fig. 5. The “enthalpy” and “entropy” component of eq. (8) for $T = T_m$ and $T = 1300$ K. A droplet will grow in the region where the entropy component is larger than the enthalpy component. The shape of the curves between the fixed values is given tentatively. The “droplet” value is assumed to hold at an n_d value where the number of interstitials in the surface layer of the droplet is about 5% of the total number n_d .

See appendix, eq. (A.7). Including this into the above considerations, even at $T = T_m$ the maximum size of a droplet is limited, rapidly decreasing with decreasing temperature. Furthermore, the interface energy between droplet and crystal, neglected in the above consideration, may influence strongly n_d^{\max} at $T \approx T_m$. From the curves at $T = T_m$ in fig. 5 and eq. (7) $\partial H_d / \partial n_d - H_I^F (1 - T/T_m)$ and $\partial S_d / \partial n_d$ at arbitrary temperatures can be derived graphically; the second set of curves is shown for $T = 1300$ K. It can be seen that n_d^{\min} tends to increase, and n_d^{\max} to decrease with decreasing temperature. Below a certain critical temperature, a droplet of any size is no longer stable.

To summarize, the concept of an interstitial agglomerate in form of a droplet requires relatively artificial assumptions, as, e.g., a very high binding entropy. Hence the identification of B-defects with droplet-like clusters of exclusively self-interstitials appears not to be very satisfactory. There are even further difficulties in connection with the droplet concept: As shown by a series of computer runs, performed for different assumptions for the droplet parameters, growth (or shrinkage) of a droplet would be so fast that even at the highest cooling rates experimentally

observed so far, a droplet would have its equilibrium size at almost any time during the cooling of the crystal. This is so because the interstitials are very mobile at high temperatures. Consequently, the size of a B-defect and in turn the size of an A-defect would be practically independent of the cooling rate – in contradiction to the observations.

The fact that the growth kinetics of a droplet is practically not influenced by the cooling rate is obviously also true for any kind of interstitial agglomerates at high temperatures. There are two possibilities to overcome these difficulties:

(i) The B-collapse model is basically wrong. However, all attempts of the present authors to establish an alternative model lead to serious contradictions with the experimental results. We therefore prefer the second possibility:

(ii) Impurities – namely carbon – determine growth kinetics as well as stability of the B-defect droplets. This assumption is suggested by the observed carbon dependence of swirl parameters as outlined in section 4.

As in the case of self-interstitials the crystal may lower its free enthalpy if a certain fraction of carbon

is incorporated into the droplet. This is so because the solubility of carbon in liquid silicon is higher than in crystalline silicon cf. ref. [43] (this argument, again, does not hold for oxygen which has about the same solubility in liquid or solid silicon). If the number of carbon atoms in the droplet influences its equilibrium size at a given temperature, as a consequence the growth kinetics of a droplet is mainly governed by the carbon diffusion, which is slow enough to result in a cooling-rate dependent growth kinetics of the droplet (the diffusion coefficient of carbon is about $1 \times 10^{-9} \text{ cm}^2 \text{ s}^{-1}$ [44]). The qualitative conclusions which can be drawn from the preceding consideration are:

(i) For the formation of a droplet a nucleus is necessary that increases in size with decreasing temperature, decreasing carbon content and decreasing supersaturation ratio of the self-interstitials.

(ii) The equilibrium size n_d^{max} of a droplet at a given temperature depends on the interstitial supersaturation *and* on the carbon content of the crystal. A decrease of anyone of these quantities leads to a decrease of the equilibrium size.

(iii) The growth kinetics of a droplet is practically governed by the carbon diffusion.

Assimilating all these items and the experimental results, we arrive at the “phase diagram” shown in Fig. 6. It should be emphasized that this diagram may give an illustration of what might happen, but by no means should be used to deduce numbers – although the axes have scales. The “life line”, i.e. the actual size of a droplet at a certain temperature, assuming a monotonic temperature decrease, is also tentatively given for high, medium and slow cooling rates. It can be seen that at high cooling rates as well as at low cooling rates, the finally frozen-in B-defect is below the detection limit.

7. The collapse of B-defects into dislocation loops and the final model

In sections 5 and 6 we discussed the change of the free enthalpy of a crystal if either a droplet or a dislocation loop is formed. In order to determine whether a collapse of a droplet into a dislocation loop

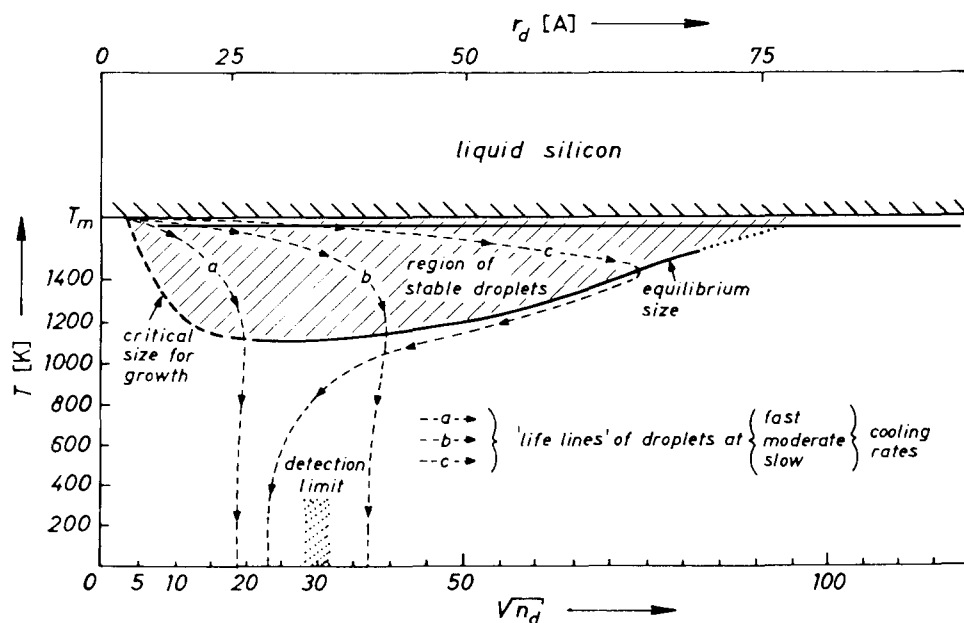


Fig. 6. “Phase diagram” of B-defects (for a certain carbon value and n (which includes n_d) constant all the time). The “life lines” give the actual size of a droplet at a certain temperature. Outside the region of stability the droplets shrink, at low temperature they are frozen in.

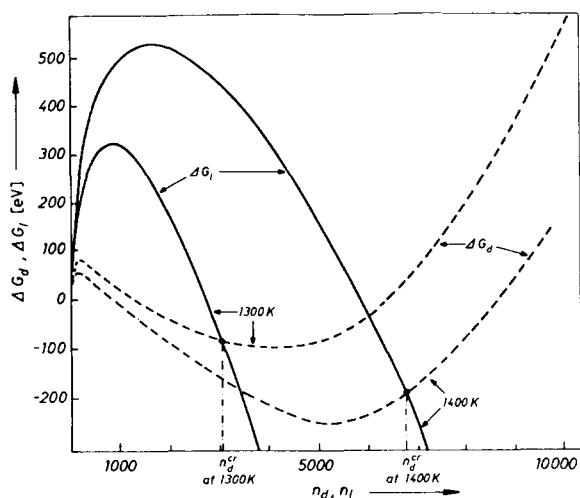


Fig. 7. Change of the free enthalpy of a crystal containing $n(T_m)$ interstitials if either a droplet or a dislocation loop is formed at a certain temperature.

takes place at all (condition: $\Delta G_d(n_d, T) \geq \Delta G_1(n_1, T)$; $n_d = n_1$), and, if this is the case, what is the critical number n_d^{cr} of interstitials in a droplet necessary for a collapse, we have to compare ΔG_d and ΔG_1 . Fig. 7

shows a ΔG_d versus n_d (ΔG_1 versus n_1) plot. The ΔG_d - n_d curves are derived from fig. 5 and eq. (7); the ΔG_1 - n_1 curves are obtained from fig. 3 and eq. (6), respectively. The point of intersection of the ΔG_d and ΔG_1 curves for a given temperature defines the critical number n_d^{cr} below which a dislocation loop would be favoured compared to a droplet and hence a droplet-loop collapse may occur. It can be seen from fig. 7 that n_d^{cr} decreases with decreasing temperature and that at high temperatures n_d^{cr} is larger than n_d^{max} (the point of intersection is placed at larger n_d values than the minimum of the ΔG_d curve, which defines n_d^{max} ; cf. the 1400 K curves of fig. 7). At high temperatures therefore droplets of any possible size are stable. From what was said in the preceding sections it may be derived that n_d^{cr} decreases with decreasing carbon content and increases with decreasing interstitial supersaturation at a given temperature.

It is noticeable that n_d^{cr} is larger than n_1^{min} , the minimum number of interstitials necessary to form a loop able to grow, provided there is no significant loss of interstitials at the surface (see section 5). This means that a dislocation loop originating from the collapse

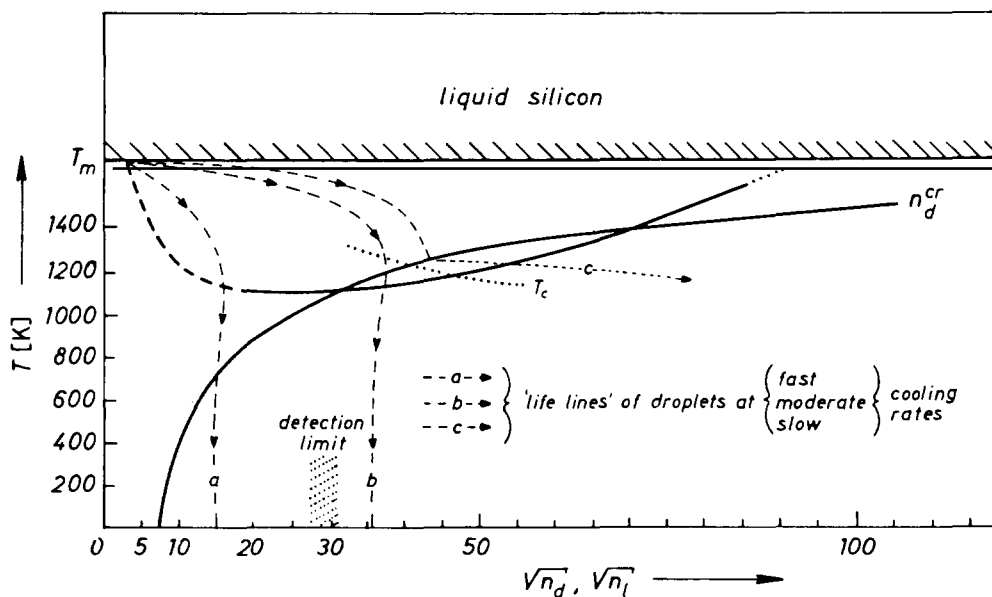


Fig. 8. Complete phase diagram for droplets and dislocation loops. n is kept constant all the time. The life lines correspond to: (a) cooling rate above 5 mm/min; small B-defects below the detection limit are frozen in; (b) cooling rate about 4 mm/min; the droplet remains (meta)stable because T is below T_c at the critical point; (c) cooling rate about 3 mm/min. The droplet collapses into a fast growing dislocation loop, A-defects are observed.

of a droplet normally will grow.

The last and most arbitrary assumption we have to make is that of thermal activation for the collapse of a B-defect. This assumption is justified by the occurrence of B-defects at all, i.e. that their collapse must have been suppressed. It is likely that large B-defects (therefore comparatively unstable) need almost no thermal activation, contrary to small (and relatively stable) droplets. We may define a critical temperature $T_c = T_c(n_d)$ below which a collapse of a B-defect (although energetically favoured) is suppressed. One may speculate about $T_c(n_d)$. However, the model operates with a large variety of T_c functions, in the following we give one curve without further justification.

Fig. 8 finally may illustrate the complete model. It contains: (i) the region of growth for a B-defect taken from fig. 6; (ii) the critical size for a collapse of a B-defect constructed according to fig. 7; (iii) the critical temperature T_c for a collapse (see above); (iv) the detection limit for B-defects (see section 6) and (v) the life lines for swirl defects at different growth rates or cooling rates, respectively. Normal growth conditions are assumed; i.e. “medium” carbon content (say, 10^{16} cm^{-3}) and a minor influence of the crystal surface on the supersaturation of the interstitials (i.e., moderate or high cooling rates). At high cooling rates the B-defects follow life line(a). They have not enough time to grow to large sizes, a collapse into an A-defect consequently does not occur. The frozen-in B-defect is even too small to be detected, the crystal seems to be swirl free. At somewhat smaller cooling rates the B-defects grow large enough to give rise to, e.g., the typical B-defect etch-pits. A-defects, however, again are not formed (life line(b)). Below a certain cooling rate a collapse at first may occur, a rapidly growing A-defect is formed (life line(c)). Not all B-defects can be expected to collapse, A- and B-defects are observed simultaneously.

8. Discussion of the experimental observations

In this section we will firstly discuss the item of section 2, in the remainder we focus on some special observations.

(i) Disappearance of swirls at high cooling rates. This issue is already discussed in its essential points in the

foregoing section. The important point is that A-defects vanish abruptly if the cooling rate exceeds a certain critical value, this is in accordance with the observations. A further increase of the cooling rate reduces the size of the B-defects below the detection limit: B-defects will also “vanish”.

(ii) Disappearance of swirls at low cooling rates. In this case a considerable fraction of interstitials is lost during the cooling by outdiffusion to the surface. The supersaturation of interstitials at a given temperature is smaller than at high cooling rates, leading to an increase in n_d^{cr} and to a decrease of the stability region of droplets. The deviations of these quantities from the normal curves is most pronounced at lower temperatures; we arrive at the diagram shown in fig. 9. At high temperatures the droplet practically assumes its equilibrium size in any moment, a life line as shown in fig. 9 may be realistic. Accordingly, A-defects are no longer formed below a certain cooling-rate and B-defects are below the detection limit.

It must be expected that this process strongly depends on the crystal diameter. So far only crystals with a diameter of 23 mm have been investigated at low cooling rates [26]. It is difficult, however, to perform similar experiments in thicker crystals, because then another mechanism may be operative, namely the formation of dislocation arrays, starting at A-defects. This was observed, e.g., in crystals with a diameter of 33 mm at $v_0 \lesssim 2 \text{ mm/min}$ [45].

(iii) Dependence of the occurrence of swirls on the cooling rate. It is evident from the experiments mentioned in item (iii) in section 2 that primarily the *cooling-rate* (and not the growth-rate) is the important parameter in swirl formation. The cooling rate is also the important parameter in our model, the experiments mentioned above are therefore intrinsically comprised in the model.

(iv) Non-appearance of B-defects in very pure crystals. This observation (together with the non-appearance of B-defects in central parts of crystals, see below) was hard to explain in a simple B-collapse model. This is so because A-defects originating from a collapse of B-defects necessarily demand the existence of B-defects. The present model, however, is able to explain this finding.

A lower carbon content of a crystal results in a smaller stability region and in a slower growth of B-defects and especially in smaller n_d^{cr} values. Further-

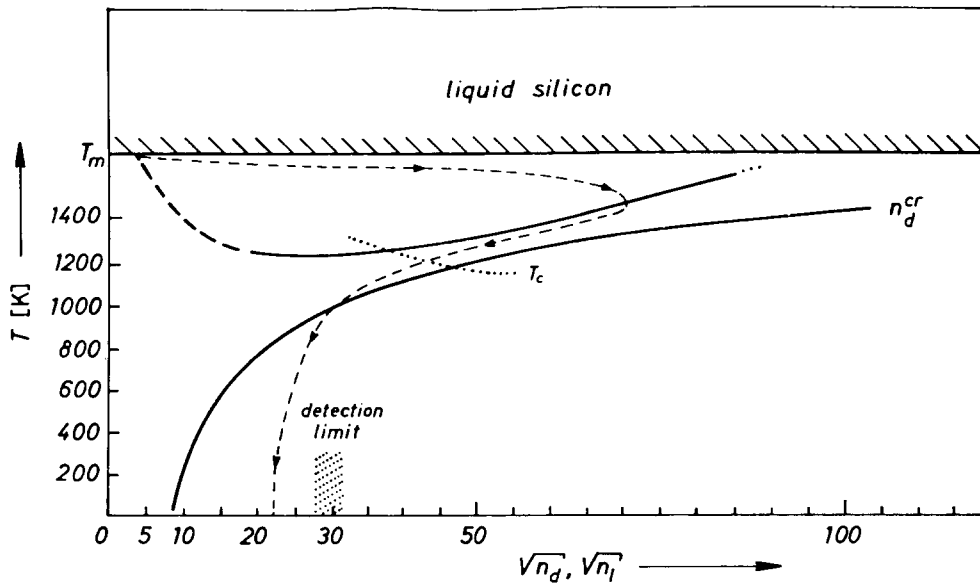


Fig. 9. Phase diagram for droplets and dislocation loops for lower supersaturation values of the interstitials. No A-defects are formed, B-defects are below the detection limit.

more, the detection limit, at least for etching, may be somewhat larger. Since droplets have almost no strain field, etching is likely to be sensitive to the carbon atoms in a B-defect. Thus a B-defect with a smaller

carbon content is harder to detect. Already small changes in the carbon concentration may change these quantities considerably. Hence we arrive at the diagram shown in fig. 10. The collapse of the droplet

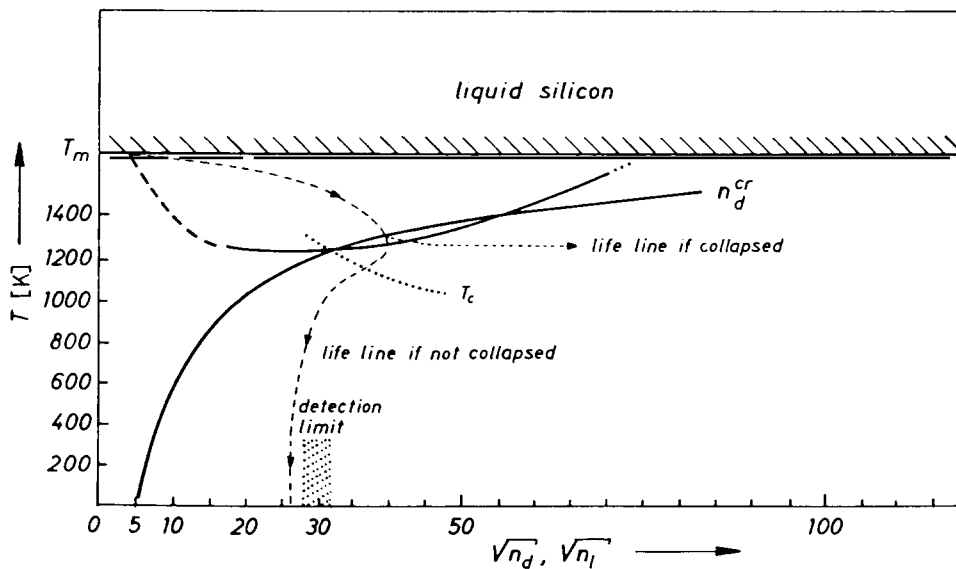


Fig. 10. Phase diagram for droplets and dislocation loops for low carbon content of the crystal. The collapse occurs at high temperatures, the freshly formed A-defects may influence the fate of the B-defects and of A-defects formed lateron.

occurs at small droplet sizes and at high temperatures. The result is at first sight a large and complicated A-defect because it has much time to grow. B-defects must not be observed for two reasons, either of which may hold separately or simultaneously: (a) The surviving B-defects are too small to be detected. (b) A freshly formed A-defect grows (if at all) very rapidly at high temperatures and thus strongly decreases the interstitial supersaturation in its neighbourhood. Nearby B-defects, not yet collapsed, therefore have an enhanced tendency to shrink, they are again below the detection limit and no longer observed.

(v) Dependence of the distances d_B and d_A between swirls and the crystal surface on the cooling rate. Near the surface two processes occur at a time: (a) The outdiffusion of interstitials, according to item (ii), leads to non-occurrence of swirls in a surface-near zone. The width of this zone increases with decreasing (low) cooling rates. (b) The higher cooling rate of near-rim regions compared to the crystal centre suppresses swirl formation as outlined in item (i). This effect is especially operative at high cooling rates; the width of the swirl-free zone thus increases with increasing (high) cooling rates. Consequently a minimum value of d_B and d_A should be observed at medium cooling rates – this is indeed found [14,26]. It is clear from this consideration that estimations of the diffusion coefficient of interstitials based on d_B , d_A or similar quantities [6,13,15,17] may only give an order of magnitude but cannot be regarded as precise values.

(vi) Lower density of B-defects in the crystal centre. The central region of a crystal differs in two ways from the outer regions. Firstly, the cooling rate is lower and secondly, the supersaturation of interstitials is higher because outdiffusion to the surface is of minor importance. Similar to what was said in the foregoing item, a reduced B-defect density may arise from the interactions between the swirl defects themselves. The first A-defect formed in a crystal region leads to a rapid decrease of the interstitial supersaturation in its neighbourhood. B-defects, or even small A-defects generated later on, thus have a strong tendency to shrink. This mechanism tends to stabilize a certain A-defect density and tends to remove B-defects. It may supply an explanation for the observation that the A-defect density is normally found to be rather insensitive to experimental parameters, pro-

vided A-defects are formed at all.

We now consider additional experiments of special interest.

In a crystal grown at 5 mm/min [46] (consequently containing no A-defects) and in a crystal grown at 0.5 mm/min [26] (consequently containing A-defects as well as B-defects), no dislocation networks are formed by growth of A-defects during a zero growth period (i.e. $v_0 = 0$) or 1 h or 18 min, respectively as it was found at medium growth rates after a zero growth period of 7 min [46]. This may be explained as follows: The incubation time of 7 min and the observation that dislocation generation always starts in the crystal centre (where the cooling rate is at lowest) indicates that the swirl loops must reach a comparatively large size before they can act as dislocation sources and that it requires a relatively long time before this size is reached. The latter might be due to a process competing with the growth of the loop; i.e. the loss of interstitials to the surface. This process obviously prevents the appropriate growth of the swirl loops at low growth rates. In the case of high growth rates, the outdiffusion during the zero growth period may even prevent the collapse of the B-defects into A-defects in the way discussed in item (ii). Further growth at 5 mm/min should result in the formation of swirl defects in a region of the crystal close to the location of the zero-growth interval. This was indeed observed by De Kock [47]. The introduction of dislocations thus can be expected to depend on the crystal diameter, in thicker crystals a lower incubation time could be expected. As already mentioned, this was indeed observed in some of our crystals, in which dislocation generation already starts at growth rates ≤ 2 mm/min (without a zero growth period), the diameter of these crystals was 33 mm. In any case the introduction of dislocations into a crystal via the growth of A-defects is still more difficult to explain than the formation of the swirls, it is therefore hard to predict whether dislocations are introduced at all, and if they are, which incubation time is necessary.

Recently, Roksnoer reported that small changes in the carbon concentration influences strongly the distance between B-defects and the solid–liquid interface during a zero growth period [48]. This distance increases with decreasing carbon content, suggesting therefore that either the growth of the B-defects is

slower, that their equilibrium size is smaller or that their formation starts at lower temperatures. In our opinion all three processes may occur simultaneously. It thus appears difficult to derive the formation temperature of B-defects from this observation. This is also true for the values of the formation temperatures of A- and B-defects given in ref. [6]; in the meantime these values have indeed been found to be in error [46,47].

One further comment should be made on the problem of the formation temperatures of swirl defects. More detailed, the question is at which temperature a nucleus large enough for the formation of a droplet (see section 6) is available (formation temperature of an B-defect) and at which temperatures the collapse of the droplets occurs (formation temperature of an A-defect). The formation temperature of the B-defects is clearly more important because the formation temperature of the A-defects depends on that. According to our model the formation of B-defects has to start at fairly high temperatures. The reason is that B-defects are not stable at low temperatures, that their growth requires some time at high temperatures and that their formation at lower temperatures is more difficult because larger nuclei are required (see section 6). It is evident, however, that the formation temperature of B-defects may be different in different crystals and certainly differs also within *one* crystal. Because only small changes in this temperature may influence strongly the further fate of a B-defect, the swirls finally observed are found in a wide variety of sizes and of complexity (see section 2). The nuclei for the B-defect formation are thought to be small associates of some carbon atoms, preferentially formed at those crystal sites where the carbon concentration reaches its maximum level. This explains the observed correlation between the carbon and the swirl distribution.

9. Final remarks and conclusions

The aim of the present paper was twofold. Firstly, the controversy between the non-equilibrium interstitial model and the equilibrium interstitial model was discussed in detail and decided in favour of the equilibrium interstitial model. Secondly, a general model for the formation of the swirl defects was proposed which accounts qualitatively for most of the swirl

experiments performed so far. The essential assumptions which were necessary were discussed in detail and, as far as presently possible, based on general thermodynamic considerations. It appears worthwhile to summarize the essential points of this model briefly.

The first and most important assumption is that A-defects may be suppressed (this follows because B-defects are generated by a collapse of B-defects, the basic idea of the B-collapse model. From this assumption it follows directly that: (i) B-defects are different in nature from A-defects; (ii) the collapse of the B-defects are observed at room temperatures), i.e., the collapse requires thermal activation to occur; and (iii) B-defects are less stable than A-defects at low temperatures. The second important assumption involves a slowly diffusing impurity atom (carbon) in both growth kinetics and stability of the B-defects. Without this assumption swirl defects would have been independent of the growth conditions, in serious contradiction to the experimental findings. The thermodynamic consideration of the A-defects is relatively simple and straight forward. For B-defects, however, more sophisticated speculations are required. The essential assumption which was made was the choice of the $\partial\Delta G_d/\partial n_d$ function shown in fig. 5. All other diagrams are essentially determined by this function and by thermodynamic relationships. Another more speculative element was the insertion of the 'life lines', but estimates of the (carbon governed) growth kinetics of a droplet justify principally the choice of this life lines.

Many questions, however, remain open. Little has been said about the nucleation of the B-defects. Provided that these nuclei are small associates of carbon atoms, directly incorporated from the melt, swirl formation should be sensitive to all growth parameters which influences amplitude and absolute value of the carbon striations (see, e.g. ref. [49]). The influence of the crystal diameter was only mentioned in special cases, effects like the "etching depression" [50], sometimes observed in thick crystals instead of swirl defects, was, e.g., not accounted for. The rôle of oxygen and other impurities was only briefly mentioned. Thus, irrespective of the large body of experiments which has been performed in the last years, much more work is required in order to arrive at a detailed understanding of the swirl phenomena.

The important conclusions which may be drawn are:

- (i) Swirl defects are a typical silicon phenomenon; similar effects in other materials (e.g., in germanium [51]) may require quite other explanations.
- (ii) In silicon special agglomerates of self-interstitials and impurity atoms (carbon) may exist, which are not simple precipitations. This may shed some light on a number of observations dealing with the generation of crystal lattice defects during oxidation or diffusion treatments of silicon [52].
- (iii) 'Swirl free' crystals may contain small B-defects. During further treatments of these crystals such virtual B-defects may give rise to a number of different phenomena. As an example, the generation of large stacking faults distributed in a typical swirl pattern is observed after an oxidation procedure of 'swirl free' crystals.

Acknowledgments

The authors are indebted to Dr. J. Burtscher, Dr. K. Mayer, Professor A. Seeger and Dr. M. Wilkins for their interest in the present work and for valuable discussions. They are especially grateful to Professor W. Frank for stimulating discussions and for critical reading of the manuscript, to Dr. W. Keller for growing the various crystals and for comments on the manuscript and to Dr. A.J.R. de Kock for making available experimental results prior to publication. The excellent technical assistance of G. Schuh who prepared the specimens and the careful photographic work of Miss L. Holl and Mrs. E. Kutschera is gratefully acknowledged.

Appendix

Let us assume that at a temperature $T < T_m$ a finite crystal region of N_0 atoms contains n_0 interstitials, n_a of which are incorporated in an interstitial agglomerate (e.g., dislocation loop or "droplet") whereas the remaining $n_0 - n_a$ interstitials are randomly distributed. Such a region may, e.g., be identified with the average volume around a swirl-defect in the investigated Si-crystals. The free enthalpy G_a of such an arrangement is given by

$$G_a = (n_0 - n_a)H_1^F - (n_0 - n_a)TS_1^F + kT \ln \frac{N_0!}{(N_0 - n_0 + n_a)!(n_0 - n_a)!} + H_a(n_a) + TS_a(n_a), \quad (\text{A.1})$$

where $H_a(n_a)$ and $S_a(n_a)$ are the enthalpy and entropy of the agglomerate, respectively.

For the determination of growth ($\partial G_a / \partial n_a < 0$) or shrinkage ($\partial G_a / \partial n_a > 0$) of the agglomerate we need the derivative of eq. (A.1) which for $N_0 \gg 1$ and $n_0 \gg 1$ is obtained as

$$\partial G_a / \partial n_a = -H_1^F + TS_1^F - kT \ln[(n_0 - n_a)/N_0] + \partial H_a / \partial n_a - T \partial S_a / \partial n_a. \quad (\text{A.2})$$

Under certain experimental conditions the number n_0 of interstitials decreases during the cooling of the crystal, e.g., due to outdiffusion of interstitials to the surface of the crystal. In this case it is convenient to rewrite eq. (A.2) in terms of the thermal equilibrium number $n_{\text{eq}}(T)$ of interstitials at temperature T ,

$$n_{\text{eq}}(T) = N_0 \exp(-H_1^F/kT + S_1^F/k), \quad (\text{A.3})$$

and the supersaturation ratio s ,

$$s = (n_0 - n_a) / n_{\text{eq}}(T), \quad (\text{A.4})$$

which leads to

$$\partial G_a / \partial n_a = -kT \ln(s) + \partial H_a(n_a) / \partial n_a - T \partial S_a(n_a) / \partial n_a, \quad (\text{A.5})$$

originally derived for vacancy agglomeration in a crystal supersaturated with vacancies [39–41]. If the outdiffusion is negligible eq. (A.5) determines the final equilibrium size of the agglomerate as a function of n_0 , N_0 and T . In connection with eq. (A.5) it is worth mentioning that an agglomerate which has already reached its final size may shrink again if s is reduced by outdiffusion to the surface or by diffusion to a nearby agglomerate of a different type. A B-defect, e.g., may get the tendency to shrink near a rapidly growing dislocation loop which considerably reduces the supersaturation of interstitials in its surroundings.

Further on we deal with the case if negligible outdiffusion and a constant number of interstitials, namely the thermal equilibrium number at $T = T_m$,

$$n_0 = n_{\text{eq}}(T_m) = N_0 \exp(-H_1^F/kT_m + S_1^F/k). \quad (\text{A.6})$$

Thus we arrive instead of eq. (A.5) at

$$\begin{aligned} \partial G_a / \partial n_a &= -H_1^F (1 - T/T_m) + \partial H_a / \partial n_a \\ &\quad - T \partial S_a / \partial n_a - kT \ln(1 - n_a/n_0). \end{aligned} \quad (\text{A.7})$$

Assuming in addition that the main amount of interstitials is still randomly distributed ($n_a \ll n_0$) we obtain

$$\begin{aligned} \partial G_a / \partial n_a &\approx -H_1^F (1 - T/T_m) + \partial H_a / \partial n_a \\ &\quad - T \partial S_a / \partial n_a. \end{aligned} \quad (\text{A.8})$$

In neglecting the term $kT \ln(1 - n_a/n_0)$, we run into difficulties only in the special case of vanishing $H_1^F (1 - T/T_m)$ and $(\partial H_a / \partial n_a - T \partial S_a / \partial n_a)$ which may occur, e.g., for large droplets at $T \approx T_m$ as described in the text. The positive \ln -term guarantees that the droplet growth stops at a finite size depending on N_0 , or in other words, on the concentration of B-defects in the crystal. Except for this special case the term $\ln(1 - n_a/n_0)$ can be neglected for the considerations in the text without arriving at wrong conclusions.

A formulation equivalent to (A.8) is given in the text for the discussion of the "droplet" thermodynamics. In the text we use ΔG_a instead of G_a . ΔG_a gives the change of free enthalpy due to the agglomeration of n_a interstitials in one agglomerate compared to the random distribution of interstitials with concentration n_0/N_0 . ΔG_a is nothing else than the n_a -dependent part of G_a from (A.1) for $n_a \ll n_0$ and may be calculated from (A.1) or by integration of (A.8) with respect to n_a . Both procedures lead to

$$\Delta G_a \approx -n_a H_1^F (1 - T/T_m) + H_a(n_a) - TS_a(n_a). \quad (\text{A.9})$$

Comparison of (A.1) and (A.9) shows that for $n_a \ll n_0$ obviously $\partial \Delta G / \partial n_a \equiv \partial G / \partial n_a$ holds which demonstrates the equivalence of (A.8) and eq. (7) in the text.

If the agglomerate is a dislocation loop the entropy term in eq. (A.8) may be neglected and we obtain for a circular faulted dislocation loop with radius r_1 , Burgers-vector b , stacking fault energy γ and shear modulus μ (see, e.g., ref. [39])

$$\begin{aligned} H_a &= H_1 = \mu [b^2 r_1 / 2(1 - \nu)] [\ln(r_1/b) + 5/3] \\ &\quad + \pi r_1^2 \gamma. \end{aligned} \quad (\text{A.10})$$

ν is Poissons ratio. Eq. (A.10) together with eq. (A.9) leads to eq. (6) in the text. The numerical values used

for the calculations are: $b = a/3\langle 111 \rangle$, $a = 5.4 \text{ \AA}$, $\gamma = 50 \text{ erg/cm}^2$, $\mu = 7.5 \times 10^{11} \text{ dyn/cm}^2$ and $\nu = 1/3$. The connection between r_1 and the number of interstitials forming the loop is

$$n_1 = \pi r_1^2 A, \quad (\text{A.11})$$

with $A = 8 \times 10^{14} \text{ atoms/cm}^2$ for the dislocation loops considered in silicon. The number of interstitial atoms in a droplet is

$$n_d = 4/3 \pi r_d^3 B, \quad (\text{A.12})$$

with $B = 4.997 \times 10^{21} \text{ atoms/cm}^3 = 1/10 \times \text{density of melt (in atoms/cm}^3)$.

References

- [1] A.J.R. de Kock, Philips Res. Rept. Suppl. No. 1 (1973).
- [2] A. Seeger, Crystal Lattice Defects 4 (1973) 221.
- [3] T.S. Plaskett, Trans AIME 233 (1965) 809.
- [4] A.J.R. de Kock, P.J. Roksnoer and P.G.T. Boonen, in: Semiconductor Silicon, Eds. H.R. Huff and R.R. Burgess (1973) p.83
- [5] F.G. Vieweg-Gutberlet, in: Semiconductor Silicon, Eds. H.R. Huff and R.R. Burgess (1973) p. 119.
- [6] A.J.R. de Kock, P.J. Roksnoer and P.G.T. Boonen, J. Crystal Growth 22 (1974) 311.
- [7] F.G. Vieweg-Gutberlet, in: Spreading Rest. Symp. Nat. Bur. Stands. Special Publ., Gaithersburg (1974) p. 185.
- [8] H.S. Grienauer, B.O. Kolbesen and K.R. Mayer, in: Lattice Defects in Semiconductors, Proc. Intern. Conf., Freiburg, 1974, Inst. of Physics Conf. Series No. 23 (1975) p. 531.
- [9] B.O. Kolbesen, K.R. Mayer and G.E. Schuh, J. Phys. E (Sc. Instr.) 8 (1975) 197.
- [10] L.I. Bernewitz, B.O. Kolbesen, K.R. Mayer and G.E. Schuh, Appl. Phys. Letters 25 (1975) 277.
- [11] P.M. Petroff and A.J.R. de Kock, Extended Abstract Electrochem. Soc., Spring Meeting Toronto 1975 (Electrochemical Soc. Princeton, NJ).
- [12] P.M. Petroff and A.J.R. de Kock, J. Crystal Growth 30 (1975) 117.
- [13] H. Föll, B.O. Kolbesen and W. Frank, Phys. Status Solidi (a) 29 (1975) K83.
- [14] H. Föll and B.O. Kolbesen, Appl. Phys. 8 (1975) 319.
- [15] P.M. Petroff and A.J.R. de Kock, J. Crystal Growth 36 (1976) 1822.
- [16] A.J.R. de Kock, in: Festkörperprobleme (Advances in Solid State Physics, Vol. 16, Ed. J. Treusch (Vieweg, Braunschweig, 1976).
- [17] A. Seeger, H. Föll and W. Frank, in: Proc. Intern. Conf. Radiation Effects in Semiconductors, Dubrovnik 1976 (in press).
- [18] N.H. Fletcher, J. Crystal Growth 28 (1975) 375.

- [19] N.H. Fletcher, *J. Crystal Growth* 35 (1976) 39.
- [20] W.W. Webb, *J. Appl. Phys.* 33 (1962) 1961.
- [21] A. Seeger and M.L. Swanson, in: *Lattice Defects in Semiconductors*, Ed. R.R. Hasiguti (Univ. of Tokyo Press, Tokyo, and Pennsylvania State Univ. Press (1968) p. 93.
- [22] A. Seeger and K.P. Chik, *Phys. Status Solidi* 29 (1968) 455.
- [23] A. Seeger, *Radiation Effects* 9 (1971) 15.
- [24] A. Seeger and W. Frank, in: *Radiation Damage and Defects in Semiconductors*, Ed. J.W. Whitehouse (The Institute of Physics, 1972) p. 262.
- [25] W. Frank, in: *Lattice Defects in Semiconductors*, Proc. Intern. Conf. Freiburg 1974, Inst. of Physics Conf. Series No. 23 (1975 p. 23.
- [26] P.J. Roksnoer, W.J. Bartels and C.W. Bulle, *J. Crystal Growth* 35 (1976) 245.
- [27] H. Föll, U. Gösele and B.O. Kolbesen, in: *Semiconductor Silicon*, Eds. H.R. Huff and E. Sirtl (1977) p. 565.
- [28] J.W. Matthews and J.A. Van Vechten, *J. Crystal Growth* 35 (1976) 343.
- [29] E. Nes, *Phys. Status Solidi (a)* 33 (1975) K5.
- [30] P.M. Petroff and A.J.R. de Kock, *J. Crystal Growth* 35, 3 (1976) 34.
- [31] K. Morizane, A. Witt and H.C. Gatos, *J. Electrochem. Soc.* 114 (1967) 738.
- [32] W. Keller, private communication.
- [33] J.D. Kamm and R. Müller, *Solid-State Electron.* 20 (1977) 105
- [34] J.A. Burton, R.C. Prim and W.P. Slichter, *J. Chem. Phys.* 21 (1953) 1987.
- [35] T. Nozaki, Y. Yatsurugi and N. Akiyama: *J. Electrochem. Soc.* 117 (1970) 1566.
- [36] Y. Yatsurugi, N. Akiyama, Y. Endo and T. Nozaki, *J. Electrochem. Soc.* 120 (1973) 975.
- [37] E. Sirtl and A. Adler, *Z. Metallk.* 52 (1961) 529.
- [38] L.I. Bernewitz and K.R. Mayer, *Phys. Status Solidi (a)* 16 (1973) 579.
- [39] G. Schoeck and W.A. Tiller, *Phil. Mag.* 5 (1960) 43.
- [40] C. Elbaum, *Phil. Mag.* 5 (1960) 55.
- [41] K.A. Jackson, *Phil. Mag.* 7 (1962) 1117.
- [42] G.V. Samsonov, Ed., *Handbook of the Physicochemical Properties of the Elements* (Plenum, New York, 1968) p. 250.
- [43] F.W. Voltmer and F.A. Padovani, in: *Semiconductor Silicon*. Eds. H.R. Huff and R.R. Burgess (1973) p. 75.
- [44] R.C. Newman and J. Wakefield, in: *Metallurgy of Semiconductor Materials*, Vol. 15, Ed. J.B. Schroeder (Interscience, New York, 1962) p. 201.
- [45] W. Keller, private communication.
- [46] A.J.R. de Kock, P.J. Roksnoer and P.G.T. Boonen, *J. Crystal Growth* 30 (1975) 279.
- [47] A.J.R. de Kock, private communication.
- [48] P.J. Roksnoer, in: Proc. First European Conf. on Crystal Growth (ECCG-1), Zürich, Sept. 1976, p. 151.
- [49] A.J.R. de Kock, P.J. Roksnoer and P.G.T. Boonen, *J. Crystal Growth* 28 (1975) 125.
- [50] W. Keller and A. Mühlbauer, in: *Lattice Defects in Semiconductors*, Proc. Intern. Conf., Freiburg 1974, Inst. of Physics Conf. Series No. 23 (1975) p. 538.
- [51] W.L. Hansen and E.E. Haller, *IEEE Trans Nucl. Sci.* NS-21 (1974) 251.
- [52] H. Föll and B.O. Kolbesen, in: *Semiconductor Silicon*, Eds. H.R. Huff and E. Sirtl (1977) p. 740.